PROCEEDINGS OF SCIENCE

Neural network identification of highly inclined muons in water-Cherenkov particle detectors

Mohsen Pourmohammad Shahvar[a,b*] , **Giovanni Marsella**[a,b], **Markus Roth**[c] and **David Schmidt**[c]

[a] *INFN sezione di Catania, Catania, Italy*

[b] *Dipartimento di Fisica e Chimica "E. Segrè" , Università degli studi di Palermo , Palermo, Italy*

[c] *Karlsruhe Institut für Technologie (KIT) Karlsruhe, Germany*

E-mail: mohsen.pourmohammadshahvar@unipa.it

This study focuses on identifying highly inclined muons in water-Cherenkov detectors similar to those used by the Pierre Auger Observatory using neural networks. Highly inclined muons, which are distinctive signatures of air showers induced by neutrinos or cosmic rays arriving at significant inclinations, offer a lower background rate compared to less inclined atmospheric particles. We explore the transition from conventional statistical approaches to machine learning methodologies to identify highly inclined muons by leveraging their unique signatures in the temporal signal distributions of three photosensors that uniformly observe the volume of a water-Cherenkov detector. By adopting machine learning, particularly neural network techniques, we aim to enhance the identification of highly inclined muons, thus improving triggering schemas designed for detecting neutrino primaries. This study not only advances the identification of highly inclined muons but also investigates the optimization of machine learning models for their efficient recognition within the water-Cherenkov detector setup.

*7th International Symposium on Ultra High Energy Cosmic Rays (*UHECR2024*)*
17-21 November 2024
Malargüe, Mendoza, Argentina

[*] Speaker

ISSN 1824-8039 . Published by SISSA Medialab.

PoS(UHECR2024)115

1. Introduction

The Pierre Auger Observatory, designed for an extensive study of cosmic rays at ultra-high energies, employs a combination of surface water-Cherenkov detectors and air fluorescence telescopes to investigate air shower phenomena comprehensively [1]–[3]. The water-Cherenkov detector design ensures robustness, cost-efficiency, and effective data acquisition for particles across a range of zenith angles [3].

1.1 Tank System

Each water-Cherenkov tank contains 12,000 liters of pure water and three photomultiplier tubes (PMTs) for detecting Cherenkov light. The surface detector array uses GPS-based positioning for accurate shower reconstruction, while its trigger system identifies events based on specific signal thresholds [3].

1.2 Muonic Showers and Triggering

The distinction between inclined and vertical muonic showers is fundamental to understanding the origins and characteristics of cosmic rays and neutrinos [4], [5]. This categorization is essential as inclined muons offer a distinct signature of air showers induced by neutrinos or cosmic rays arriving at substantial inclinations, presenting an opportunity to minimize background noise and enhance the sensitivity of astroparticle measurements [6], [7].

Identifying highly inclined muons in water-Cherenkov detectors traditionally relies on empirical methods, but these struggle to distinguish muons from noise, necessitating improved approaches [8].

The Unified Readout Board (UUB) processes Cherenkov signals from PMTs for efficient data acquisition[9], [10]. A hierarchical trigger system, employing “Threshold” (TH) and “Time-over-Threshold” (ToT) triggers, filters significant muonic events while reducing background noise [11] [12]. By refining detection through VEM and ToT criteria, the system enhances cosmic ray shower reconstruction, advancing astroparticle physics [13].

1.3 The Baseline Model

The baseline model acts as a vital benchmark, helping us understand how well our current methods work and providing a reference point for assessing any improvements or changes.

The current trigger threshold (i.e., Our Baseline Model) of 3.2 Vertical Equivalent Muon (VEM) [11] in the Pierre Auger setup, while traditionally employed, presents notable limitations. This threshold denotes the minimum signal amplitude required to initiate the detection process, with VEM serving as a standardized unit for comparative analysis. However, the visualization of the data indicates a conspicuous dearth of detected events under this stringent criterion, rendering the acquired information sparse and inadequate for comprehensive analysis.

2. Muon Simulation and Feature Extraction

To enhance muon identification in water-Cherenkov detectors, we simulated over 100,000 single muon events in a tank equipped with three symmetrically placed photomultiplier tubes (PMTs) to capture Cherenkov radiation. These simulations, varying in spatial coordinates and directions, enabled the analysis of zenith and azimuth angles, revealing the transition from vertical to inclined muons across a 0–90° zenith angle range.

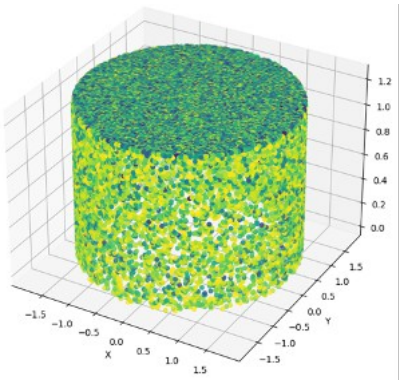

Figure 1: Simulated tank under muon injections

Preprocessing involves extracting key features from the raw PMT signals to enhance the accuracy of muon identification. These features include the **highest peak values**, which represent the maximum signal amplitude and help in distinguishing strong particle interactions; the **integrals of PMT traces**, which provide a measure of the total signal energy over time, capturing the overall intensity of the Cherenkov light; and the **rise times**, which reflect the speed at which the signal reaches its peak, offering insights into the timing and dynamics of the muon's passage through the detector. Together, these features encapsulate critical information to forming the basis for effective signal classification.

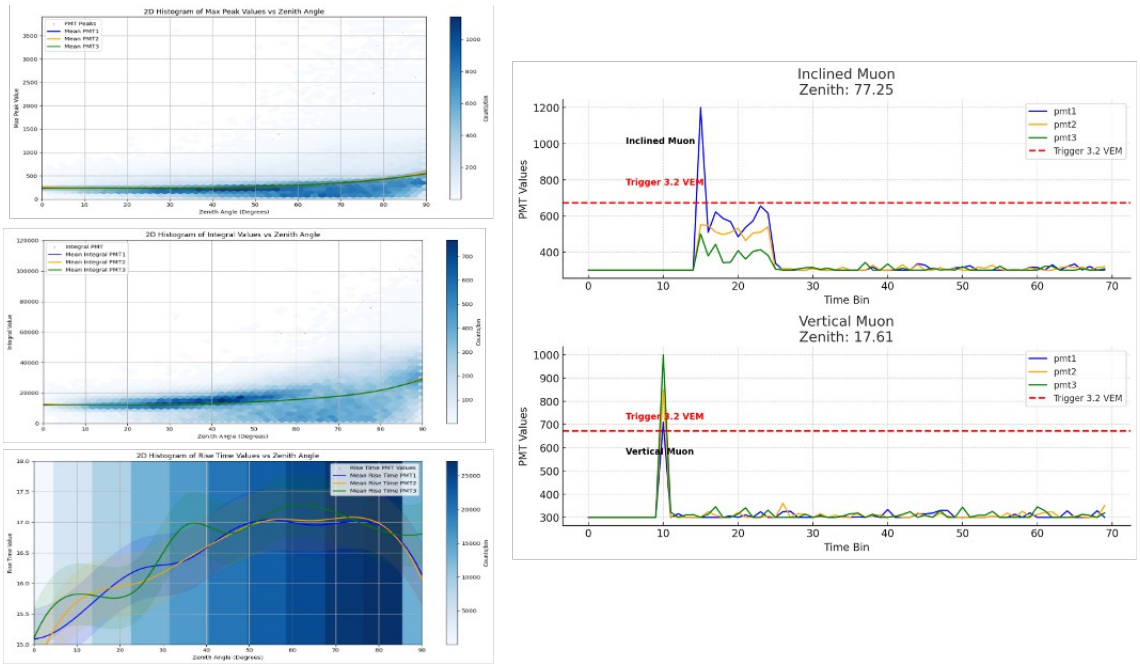

Figure 2: Feature Selection phase through the Vertical and Inclined Muon Events

3. Machine Learning Paradigm

This study evaluates neural networks, including ResNet and LSTM, for detecting inclined muons. Hybrid models like ResNet-XGBoost and LSTM-XGBoost capitalize on the strengths of sequential and gradient-boosting frameworks. These models effectively handle the complexities of PMT signal data, enabling precise muon classification.

3.1 1st Hybrid Approach: Integrating XGBoost-LSTM with Random Forest Regressor

The hybrid XGBoost-LSTM approach, enhanced with a Random Forest Regressor, combines the strengths of gradient boosting, sequential modeling, and ensemble learning to improve muon identification in water-Cherenkov detectors. LSTM captures long-range dependencies in PMT data, while XGBoost handles complex datasets and mitigates overfitting. The Random Forest further boosts accuracy by aggregating predictions across decision trees. The hybrid model architecture integrates LSTM and XGBoost outputs through a concatenate layer, producing a refined prediction of Zenith Angles. Careful distribution of Zenith Angles in training and testing datasets ensures balanced representation and robust generalization across all scenarios. This approach significantly enhances classification accuracy, robustness, and interpretability, contributing to advancements in muon detection and astroparticle physics.

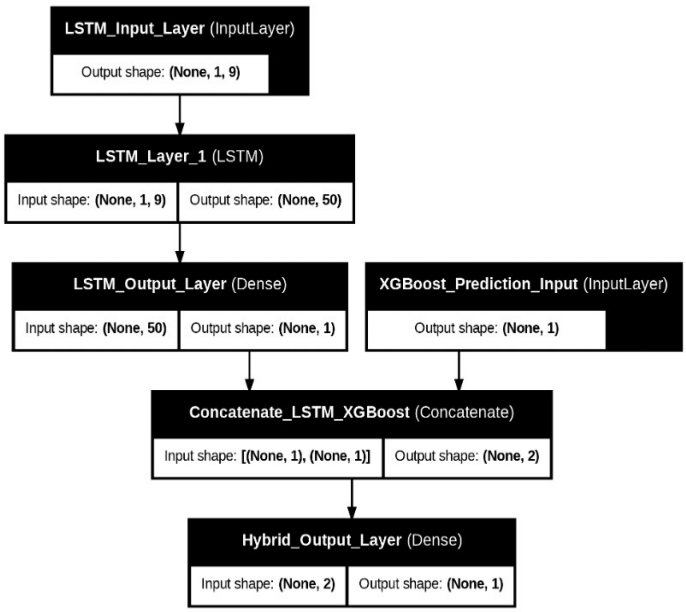

Figure 3: Hybrid Model Architecture (LSTM+XGBoost)

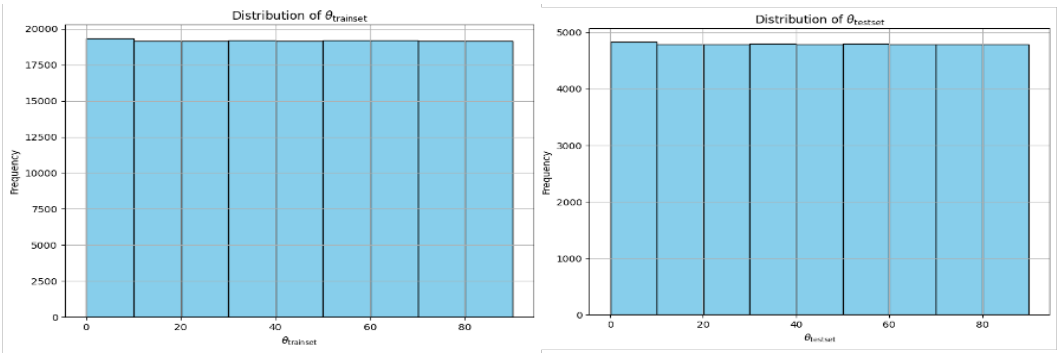

Figure 4: Train/Test set of Zenith Angle distribution

The 2D histogram illustrates the relationship between true and predicted Zenith Angles for the hybrid model. A color gradient indicates prediction density, with blue regions showing lower densities and red regions highlighting higher densities. The dashed line represents perfect predictions, where true zenith and predicted zenith angles are equal. Data clustering along this

line, especially in lower and mid-range angles, demonstrates high accuracy and precision. Red high-density areas near the line further confirm the model's consistent performance. The model effectively captures Zenith Angles above 60°, crucial for studying inclined events. Deviations from the line reflect minor errors, which are more spread at higher angles. Overall, the model exhibits robust accuracy across a wide range of angles.

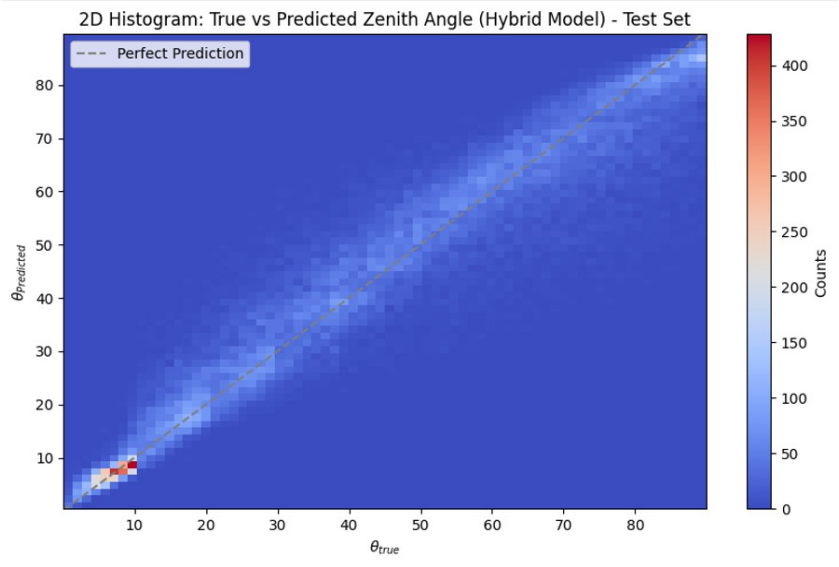

Figure 5: True Zenith Vs. Predicted Zenith for the first Hybrid model

Performance evaluation shows the hybrid model achieving the lowest MSE (58.37) and MAE (5.32), outperforming XGBoost (MSE: 126.06, MAE: 8.04) and LSTM (MSE: 323.07, MAE: 13.719), demonstrating its superior prediction capability.

3.2 2ndHybrid Approach: Integrating XGBoost-ResNet with Random Forest Regressor

The second hybrid model integrates ResNet, XGBoost, and a Random Forest Regressor, leveraging ResNet's hierarchical feature extraction and XGBoost's gradient boosting for robustness, while the Random Forest ensures stability through ensemble learning. This architecture (Figure 6A) effectively captures both high-level features and non-linear data relationships, optimizing Zenith Angle predictions.

The 2D histogram in Figure 6B shows a strong alignment of predictions with the perfect prediction line, particularly for highly inclined Zenith Angles above 60°, demonstrating the model's capability to capture rare extreme-angle events. This clustering, especially at low and high angles, highlights its robustness and comprehensive coverage in muon trajectory analysis.

Performance comparisons confirm the hybrid model's superiority with the lowest error metrics (RMSE: 7.98, MSE: 63.75, MAE: 5.65), significantly outperforming ResNet (RMSE: 16.45, MSE: 270.78, MAE: 12.46) and XGBoost (RMSE: 11.22, MSE: 126.06, MAE: 8.04). This demonstrates its robustness and accuracy in complex prediction tasks.

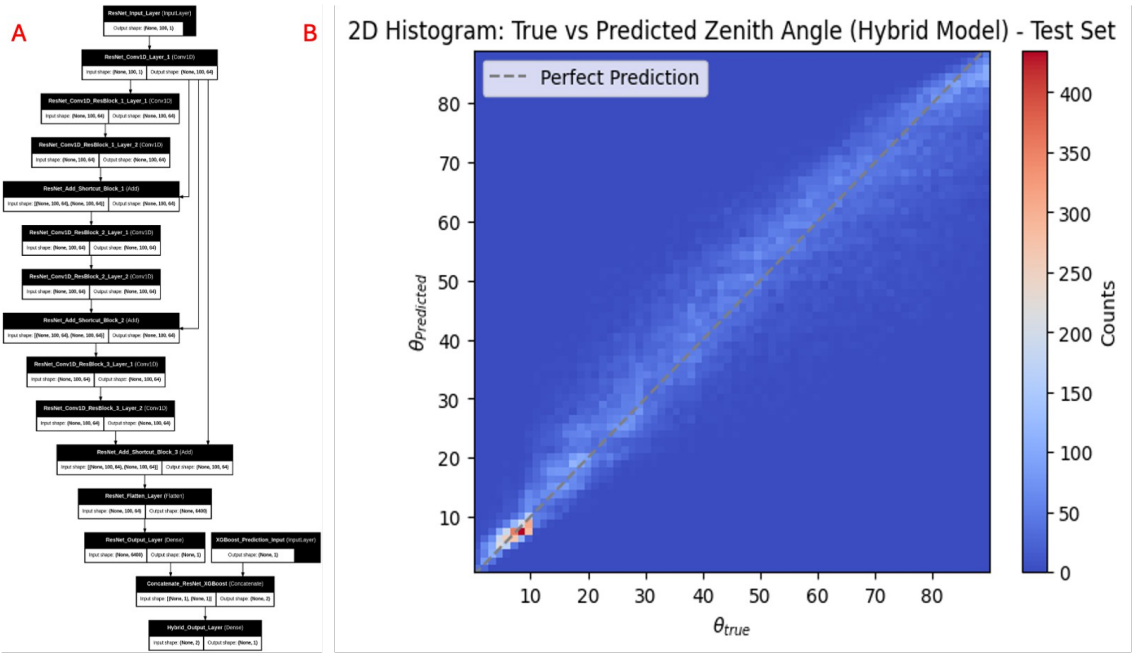

Figure 6: A) ResNet+XGB Hybrid model, B) True Vs. Predicted Zenith Angle of Hybrid model

4. Comparative Evaluation of Hybrid Models for Zenith Angle Prediction

The bar plot in Figure 7 compares the performance of LSTM-XGBoost and ResNet-XGBoost hybrids across RMSE, MSE, and MAE metrics. The LSTM-XGBoost hybrid consistently outperforms the ResNet-XGBoost hybrid, achieving the lowest RMSE (7.64) and MAE (5.32), indicating superior accuracy and smaller residual errors. ResNet-XGBoost follows closely with RMSE (7.98) and MAE (5.65), demonstrating slightly less precision. Both hybrid models significantly outperform their standalone components (LSTM and ResNet), with XGBoost as a consistently strong base model. These results emphasize the accuracy gains from hybridization, with LSTM-XGBoost achieving the best overall precision.

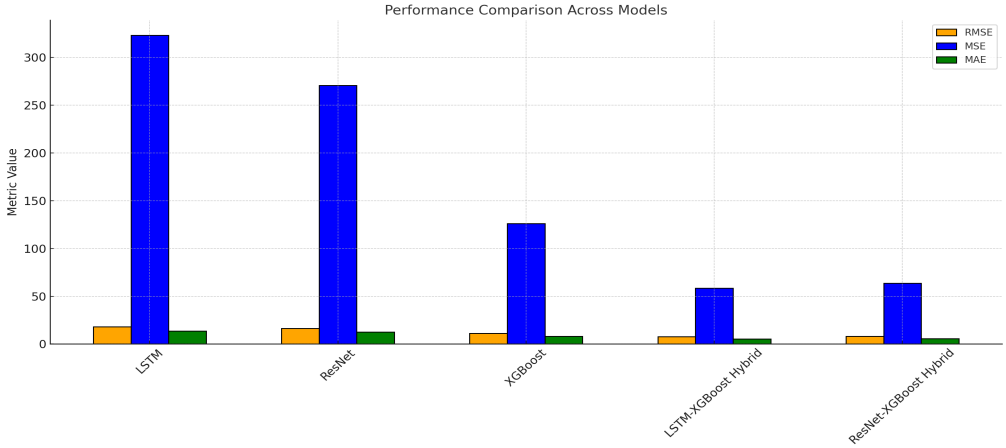

Figure 7: Comparative Evaluation of Hybrid Models for Zenith Angle Prediction

4.1 Purity and Efficiency of Hybrid Model

The metrics of purity and efficiency serve as critical benchmarks for evaluating the performance of predictive models. These metrics are particularly pertinent when analyzing hybrid models applied to specific event channels, such as the Neutrino Channel.

4.1.1 Purity Vs. Efficiency for Hybrid Model (LSTM + XGBoost)

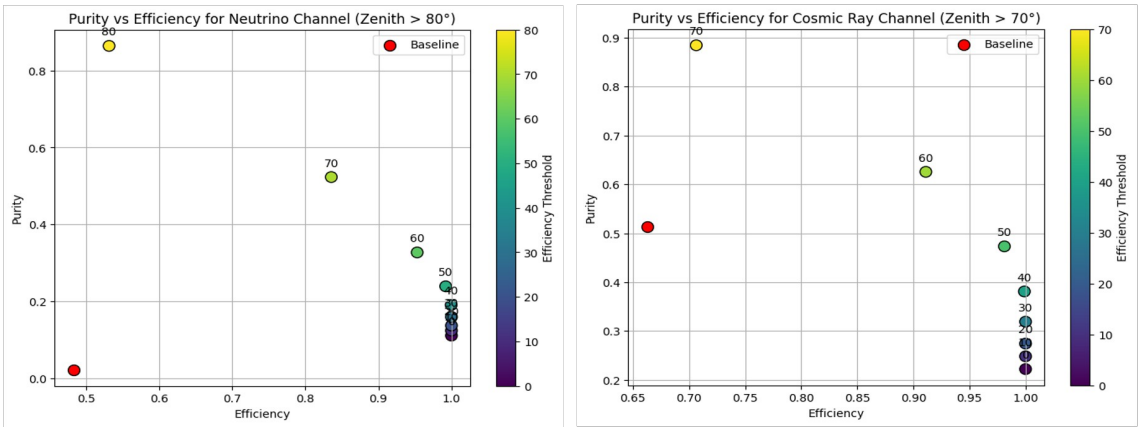

Figure 8: Left: Purity vs. Efficiency for Neutrino Channel (Zenith > 80°), Right: Purity vs. Efficiency for Cosmic Ray Channel (Zenith >70°)

The Hybrid LSTM-XGBoost model outperforms the baseline 3.2 VEM trigger system for Neutrino Channel events with Zenith Angles above 80°, achieving significantly higher purity without compromising efficiency. The efficiency threshold gradient highlights the model's superior detection optimization across various angles. In the Cosmic Ray Channel (Zenith Angles above 70°), the hybrid model demonstrates a clear advantage over the baseline, which struggles with performance. Particularly between 60° and 70°, the hybrid model excels in balancing purity and efficiency, reinforcing its effectiveness in optimizing cosmic ray event detection.

4.1.2 Purity Vs. Efficiency for Hybrid Model (ResNet + XGBoost)

The Hybrid ResNet-XGBoost model outperforms the baseline trigger for the Neutrino Channel by maintaining high purity without sacrificing efficiency, addressing the baseline's vulnerability to false positives at high efficiency. Its smooth gradient response from 0° to 80° demonstrates adaptability in detecting neutrino events, particularly at high Zenith Angles. Figure 9 (right) further highlights its superiority, showing a marked improvement in purity and efficiency near the 70° threshold, effectively reducing noise and isolating cosmic ray events. The model's ResNet backbone ensures consistent performance across thresholds, reinforcing its stability and precision in detecting high Zenith Angle cosmic rays.

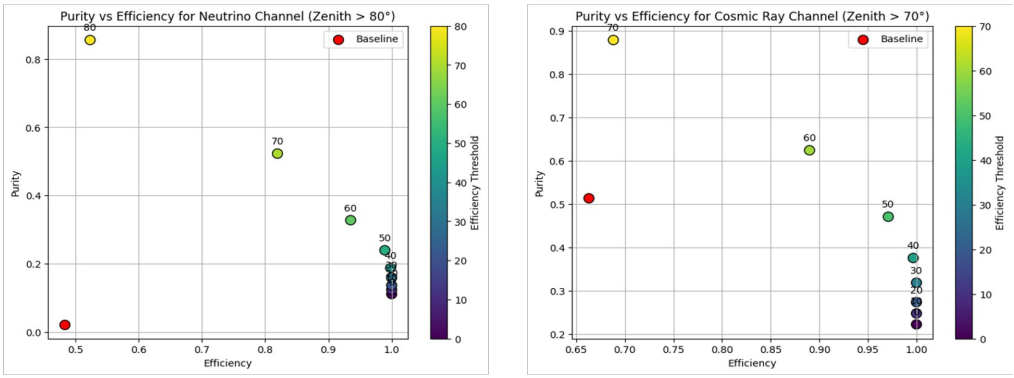

Figure 9: Left: Purity vs. Efficiency for Neutrino Channel (Zenith > 80°), Right: Purity vs. Efficiency for Cosmic Ray Channel (Zenith > 70°)

5. Conclusion

Both hybrid models outperform the baseline, exposing the 3.2 VEM trigger system's limitations in handling high Zenith Angle events. The Hybrid LSTM-XGBoost demonstrates exceptional adaptability, enhancing detection accuracy through sequential data analysis, while the Hybrid ResNet-XGBoost provides robust performance with consistent purity-efficiency gains across thresholds. The Neutrino Channel shows the most significant improvements, handling rare, high-inclination events, while the Cosmic Ray Channel benefits from noise reduction and precise high-energy particle identification. These results emphasize the transformative potential of hybrid machine learning models in advancing astrophysical event detection.

6. References

[1] A. Abdul Halim *et al.*, "Constraining the sources of ultra-high-energy cosmic rays across and above the ankle with the spectrum and composition data measured at the Pierre Auger Observatory," *J. Cosmol. Astropart. Phys.*, vol. 2023, no. 05, p. 024, May 2023, doi: 10.1088/1475-7516/2023/05/024.

[2] The Pierre Auger Collaboration, "First Estimate of the Primary Cosmic Ray Energy Spectrum above 3 EeV from the Pierre Auger Observatory," Jul. 2005, [Online]. Available: http://arxiv.org/abs/astro-ph/0507150.

[3] I. Allekotte *et al.*, "The surface detector system of the Pierre Auger Observatory," *Nucl. Instruments Methods Phys. Res. Sect. A Accel. Spectrometers, Detect. Assoc. Equip.*, vol. 586, no. 3, pp. 409–420, Mar. 2008, doi: 10.1016/j.nima.2007.12.016.

[4] I. Valiño, J. Alvarez-Muñiz, M. Roth, R. A. Vazquez, and E. Zas, "Characterisation of the electromagnetic component in ultra-high energy inclined air showers," *Astropart. Phys.*, vol. 32, no. 6, pp. 304–317, Jan. 2010, doi: 10.1016/j.astropartphys.2009.09.008.

[5] P. Abreu *et al.*, "Search for photons above 10 19 eV with the surface detector of the Pierre Auger Observatory," *J. Cosmol. Astropart. Phys.*, vol. 2023, no. 05, p. 021, May 2023, doi: 10.1088/1475-7516/2023/05/021.

[6] J. Abraham *et al.*, "A study of the effect of molecular and aerosol conditions in the atmosphere on air fluorescence measurements at the Pierre Auger Observatory," *Astropart. Phys.*, vol. 33, no. 2, pp. 108–129, Mar. 2010, doi: 10.1016/j.astropartphys.2009.12.005.

[7] K.-H. Kampert, M. Alejandro Mostafa, and E. Zas, "Multi-Messenger Physics With the Pierre Auger Observatory," *Front. Astron. Sp. Sci.*, vol. 6, Apr. 2019, doi: 10.3389/fspas.2019.00024.

[8] The Pierre Auger Collaboration *et al.*, "The Fluorescence Detector of the Pierre Auger Observatory," Jul. 2009, doi: 10.1016/j.nima.2010.04.023.

[9] R. Sato *et al.*, "AugerPrime implementation in the DAQ systems of the Pierre Auger Observatory," in *Proceedings of 38th International Cosmic Ray Conference — PoS(ICRC2023)*, Aug. 2023, p. 373, doi: 10.22323/1.444.0373.

[10] The Pierre Auger Collaboration *et al.*, "AugerPrime Surface Detector Electronics," Sep. 2023, [Online]. Available: http://arxiv.org/abs/2309.06235.

[11] J. Abraham *et al.*, "Trigger and Aperture of the Surface Detector Array of the Pierre Auger Observatory," Nov. 2011, doi: 10.1016/j.nima.2009.11.018.

[12] T. Huege, "The Radio Detector of the Pierre Auger Observatory – status and expected performance," *EPJ Web Conf.*, vol. 283, p. 06002, Apr. 2023, doi: 10.1051/epjconf/202328306002.

[13] D. Allard *et al.*, "The trigger system of the Pierre Auger Surface Detector: operation, efficiency and stability," Oct. 2005, [Online]. Available: http://arxiv.org/abs/astro-ph/0510320.